Tellus (1985), *37B*, 64–77

Calculation of ground temperature and fluxes by surface models: a comparison with experimental data in the African savannah

By G. CAUTENET, Y. COULIBALY, *Faculté des Sciences, Département de Physique, (04) B.P. 322 Abidjan (04) Côte d'Ivoire,* and Ch. BOUTIN, *L.A.M.P.-I.O.P.G., Université de Clermont-Ferrand II, B.P. 45, 63170, Aubière, France*

(Manuscript received February 23; in final form November 7, 1984)

ABSTRACT

In large-scale models, an accurate calculation of energy fluxes at the lower boundary is important to ensure satisfactory predictions of the meteorological parameters. This work is performed using surface models.

In this paper, various surface models, previously studied by Deardorff are tested against experimental data from the West African Monsoon Experiment 1979 in the Ivory Coast. Physical properties of the soil are assumed constant and uniform. Input variables are dry and wet bulb temperatures, wind velocity at the 2 m level, and global radiation. We compute sensible and latent heat fluxes and the surface conduction flux. A Crank-Nicholson scheme has been used with a time step of 5 min. Estimated sensible and latent heat fluxes agree well with experimental data. The order of magnitude of the difference between theoretical and experimental values is 30 W m^{-2} for evaporation and 20 W m^{-2} for sensible heat. Surface soil heat flux ie less satisfactorily calculated, which could result from properties assumed constant such as soil surface humidity. A model including the heat conduction in the soil provides the best results. The others, based on empirical formulations of surface soil heat flux, are less satisfactory. However, with a simple two-layer model, the predictions are quite acceptable.

1. Introduction and a presentation of the data set

A review of several simple empirical surface models of current use was made by Deardorff (1978). Due to lack of measurements, he evaluated these models by comparison with a more complex reference model including a heat diffusion equation in the soil. This model is referenced here as the "multi-layer model". The empirical models are based on the calculation of soil surface temperature from the heat budget equation in the upper layer of the soil (Washington and Williamson, 1977; Laval et al., 1978). They are referenced as "empirical" because of somewhat *a priori* formulations of the ground heat flux. The multi-layer model is one-dimensional. It is assumed that the soil properties are constant and uniform, with bare surface (no vegetation). These assumptions are current in general circulation models. As they are rather crude, it is important to yield an estimate of the bias they could involve: the qualification of ground surface models in varied conditions is a necessary step before dealing with the still pending problem of the large-scale model sensitivity to possible lack of accuracy in these ground models. There is not yet much information in the literature about this sensitivity. However, under unstable conditions, the boundary layer parameters are strongly influenced by ground properties such as surface albedo or moisture (Zhang and Anthes, 1982). These parameters control the absorbed radiation at the ground and surface evaporation respectively.

This paper deals with the direct comparison of the multi-layer and the empirical models with experimental data. The spatial extent of this study

is a field with a fetch of some hundred metres (a single site of data collection) but it should be noted that such measurements are very rare in the African savannah.

Experimental data have been collected on a sub-sahelian savannah site (Korhogo, 9°30′N, 5°30′W, about 400 m above sea level, in the Northern Ivory Coast) during WAMEX (West African Monsoon Experiment) in 1979 by the Laboratoire Associé de Météorologie Physique (L.A.M.P., Université de Clermont-Ferrand II, France). The experimental area was partly covered with grass (about 30 cm high). The experimental device consisted of a 6 m high mast with three measurement levels: 50 cm, 2 m and 6 m. The following data were recorded: wind speed (cup anemometers), temperature and humidity (dry and wet bulb ventilated thermometers), wind direction (at the top of the mast). Moreover, six thermocouple gauges measured the soil temperatures at depths of 0, 5, 10, 20, 40 and 80 cm. Global radiation was measured by a Kipp pyranometer. The set of instruments was completed by a rain gauge. The data were recorded on a magnetic tape with a period of 5 min. More details can be found in Hervier et al. (1979).

Table 1. *Rainfall (mm) recorded from July 1 to August 10 at Korhogo during WAMEX 1979*

July		July		July		August	
day	rainfall	day	rainfall	day	rainfall	day	raintall
1	0.0	11	4.7	21	0.0	1	0.0
2	0.0	12	0.0	22	0.2	2	0.0
3	6.6	13	0.0	23	55.6	3	0.2
4	0.2	14	4.8	24	15.8	4	0.0
5	1.7	15	0.0	25	0.2	5	24.0
6	9.9	16	0.0	26	17.9	6	0.0
7	0.1	17	5.0	27	0.0	7	0.0
8	0.0	18	31.8	28	9.8	8	0.0
9	0.0	19	87.0	29	0.0	9	0.0
10	0.3	20	0.0	30	6.1	10	0.0
				31	25.4		

The tapes were processed with a Hewlett-Packard 21 MX computer. 25 min average values were calculated. The sensible and latent heat fluxes were estimated with the aerodynamic method (Saugier and Ripley, 1978). Assuming that the soil

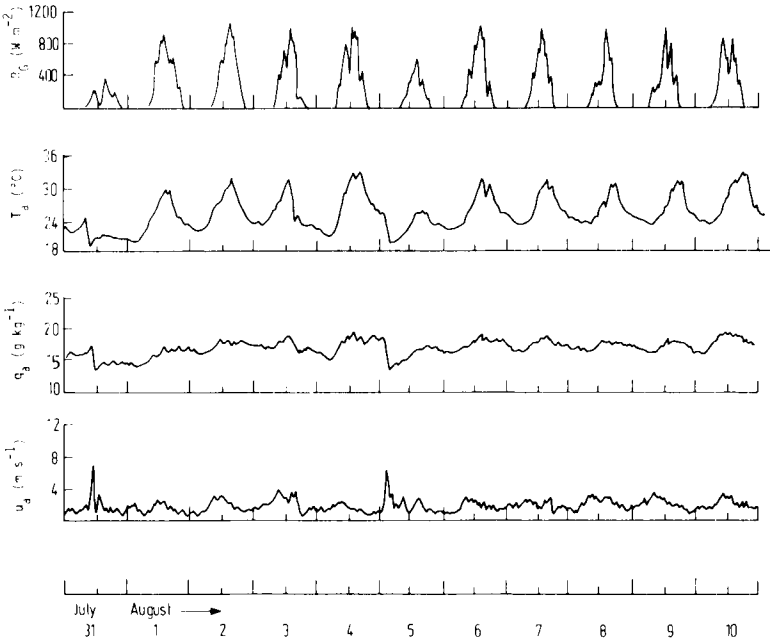

Fig. 1. Meteorological parameters during the period July 31 to August 10 (1979) at Korhogo: R_G = global radiation; T_a = air temperature at 2 m above ground; q_a and u_a = respectively specific humidity and wind speed at the same level (2 m).

heat flux becomes quite negligible at a depth of 80 cm, the surface value of this flux, G_0, is given by the integral:

$$G_0 = C \int_0^{z_2} \frac{\partial \theta_e}{\partial t} \, dz \qquad (z_2 = 80 \text{ cm}), \tag{1}$$

where θ_e is the experimental soil temperature profile and C the specific heat of soil, assumed constant and uniform. A continuous set of 11 days has been used in this work. The soil parameters such as thermal conductivity, specific heat and wetness, and surface properties such as albedo and emissivity were not directly measured. The investigated period (July 31 to August 10, 1979) took place in the middle of the rainy season. This period is characterized by an alternation of rainy days (squall lines on July 31 and August 5) and sunny days. Wind speeds are generally very low. Aside from occasional disturbances, they are lower than 4 m s^{-1}. Values ranging between 2 and 3 m s^{-1} are frequently observed. During daytime, instability is strong: the Richardson number may be as low as −0.5. Rainfalls from July 1 to August 10 are presented in Table 1. Fig. 1 summarizes the main meteorological features from July 31 to August 10. A detailed description of this period has been presented by Coulibaly (1981).

2. Description of the models

2.1. The atmospheric surface layer

The description below is common to all models.

In the lowest part of the atmosphere (where the fluxes are assumed conservative) the various terms of the heat budget equation (except G_0) may be expressed by bulk formulas:

$$H = \rho_a C_p C_{h0} u_a(\theta_0 - T_a) \tag{2a}$$

$$\text{LE} = L\rho_a C_{h0} u_a(q_0 - q_a) \tag{2b}$$

q_0 is interpolated from $q_{sat}(\theta_0)$ and q_a in the following manner:

$$q_0 = \alpha q_{sat}(\theta_0) + (1 - \alpha) q_a, \tag{3}$$

so that eq. (2b) becomes:

$$\text{LE} = L\rho_a C_{h0} u_a \alpha(q_{sat}(\theta_0) - q_a). \tag{4}$$

Since the models do not take the soil water budget into account, the parameter α which characterizes the soil wetness near the surface is kept constant. A test prohibits q_0 from becoming greater than $q_{sat}(\theta_0)$ when condensation occurs (at that time, α equals 1).

The infrared budget is given by the Angström formula:

$$R_{IR} = f(v)(R_T - \varepsilon_s R_L), \tag{5}$$

where

$$R_T = \varepsilon_s \sigma \theta_0^4, \tag{6}$$

$$R_L = (0.82 - 0{\cdot}25 \cdot 10^{-0.052 e_a}) \sigma \bar{T}_a^4. \tag{7}$$

$f(v)$ accounts for the effect of cloudiness v. It is assumed that

$$f(v) = 1 - 0.55v \tag{8}$$

(Budyko, 1974; Reed and Halpern, 1975; Coulibaly, 1981). A rough estimate of cloudiness is derived from the formula:

$$R_G = R_{G0}(1 - C_1 v), \tag{9}$$

from which v is deduced:

$$v = (R_{G0} - R_G)/C_1 R_{G0}, \tag{10}$$

where R_{G0} is the global radiation when the sky is clear. This value is estimated by astronomic formulas (Paltridge and Platt, 1978), with an atmospheric attenuation of 20%. Adjustment runs lead to a value of 0.8 for C_1.

2.2. The soil

2.2.1. The multi-layer model. In a medium with uniform physical properties, the heat conduction equation is

$$\frac{\partial \theta(z,t)}{\partial t} = \kappa \frac{\partial^2 \theta(z,t)}{\partial z^2}. \tag{11}$$

The lower boundary condition is $\theta = \theta_\infty$. This parameter is equal to the value of the temperature at 80 cm depth. For a 24-h period, it remains practically constant. At the soil-atmosphere interface, the heat budget equation, which accounts for no heat storage in a thin film at soil surface, provides the upper limit condition for the diffusion equation:

$$H + \text{LE} + R_{IR} - (1 - A) R_G + G_0 = 0. \tag{12}$$

The surface soil heat flux by conduction is found from

$$G_0 = -\lambda(\partial\theta/\partial z) \qquad \text{at } z = 0. \tag{13}$$

The input data for the model are:

the wind velocity at 2 m,

the wet and dry bulb temperatures at 2 m,

the global radiation (surface value).

Eq. (11) is discretized following the Crank-Nicholson scheme. There are ten levels in the one-dimensional grid used in the integration: these levels correspond to depths expanding exponentially (except the last): 0 (surface), 6 mm, 12 mm, 25 mm, 5 cm, 10 cm, 20 cm, 40 cm, 80 cm, 1 m. The time step Δt is constant and equal to 5 min. Tests on Δt, allowed by the implicit character of the scheme, showed negligible truncation errors (a run with $\Delta t = 30$ s was performed with results very close to those obtained with $\Delta t = 5$ min). The non-linear terms are linearized as follows:

$$q_{sat}[\theta(t+\Delta t)] = q_{sat}[\theta(t)] + [\theta(t+\Delta t) - \theta(t)] \times \left[\frac{\partial q_{sat}}{\partial \theta}\right]_{\theta(t)}, \quad (14)$$

$$\theta^4(t+\Delta t) = 4\theta^3(t)\,\theta(t+\Delta t) - 3\theta^4(t). \quad (15)$$

2.2.2. The empirical models. The five empirical models previously tested by Deardorff are evaluated here by direct comparison with the experimental data. They are based upon solving the heat budget equation (12). G_0 is expressed in various ways, which distinguishes one model from another. According to the expression chosen, they are referenced as 1, 2, 3, 4 or 5. The different formulas for G_0 are described thereafter:

model 1: $G_0 = 0$; (16a)

model 2: $G_0 = \frac{1}{3}H$ (16b)

model 3:

$$\begin{cases} G_0 = -0.19R_N & \text{when} \quad R_N < 0 \text{ (day)} \\ G_0 = -0.32R_N & \text{when} \quad R_N > 0 \text{ (night);} \end{cases} \quad (16c)$$

model 4: $G_0 = \pi^{-1/2}\, Cd_1(\partial\theta_0/\partial t)$ (forcing process); (16d)

model 5: $G_0 = 0.5\pi^{-1/2}\, Cd_1(\partial\theta_0/\partial t) + Cd_1\pi^{1/2}\,\dfrac{\theta_0 - \theta_\infty}{\tau}$. (16e)

This last model, called by Deardorff "force-restore model", is characterized by two layers: the surface of the ground and an inner level (at depth d_1) at which the temperature is θ_∞. Eqs. (16a) to (16e) are linearized, using for $\partial\theta_0/\partial t$ the analog $(\theta_{0|n+1} - \theta_{0|n})/\Delta t$ (the subscript $n+1$ refers to the present, unknown time step, and n refers to the past time step). All the terms of the heat budget equation (except G_0) are expressed in the same way as for the multi-layer model. The input data are the same as for the multi-layer model.

3. Initial choice of the basic parameters

The basic parameters A, κ, λ, α, C_{h0} and ε_s have been chosen by adjustments. An initial choice of these parameters is performed as follows:

albedo A: 0.20 (Rockwood and Cox, 1978).

κ and λ: in agreement with measurements in the laterite, a value for κ of $0.7 \cdot 10^{-6}$ m^2 s^{-1} was taken (Baudet and Degiovanni, personal communication). An estimate of λ is derived from the specific heat C taken as $2.2 \cdot 10^6$ J kg^{-1} K^{-1} by Coulibaly for the processing of the WAMEX data used here. From these values of κ and C, an initial value of 1.5 W m^{-1} K^{-1} has been selected for λ. These values agree with De Vries data (1966) for wet soils.

$\alpha = 0.5$ (the soil was very wet).

$C_{h0} = 5 \cdot 10^{-3}$. This value agrees with a rough estimate from the formula:

$$C_{h0} = u_* T_* / (u_a(\theta_0 - T_a)) \quad (17)$$

(u_* and T_* are the scaling surface parameters for momentum and sensible heat). Typical values of u_*, T_*, u_a and $\theta_0 - T_a$ are, respectively, 0.3 m s^{-1}, 0.3 K, 2 m s^{-1} and 10 K, so that C_{h0} is about $5 \cdot 10^{-3}$. Formula (17) is obtained if we compare the expression of H from the aerodynamic method, i.e. $\rho_a C_p T_* u_*$ (Saugier and Ripley, 1978) with the bulk formula (2a). (This estimate of C_{h0} by formula (17) is rather crude because no measurements of H by some other method than the aerodynamic were available).

In order to study the effects of changing these values, sensitivity runs have been performed for a typical day (August 7). Some examples are given in Figs. 2 and 3, for the maximum values of the surface temperature θ_0 issued from the multi-layer model, referenced at T_{surf}^{max} MLM, and from model 5 (two-layer model), referenced as T_{surf}^{max} 2LM. The

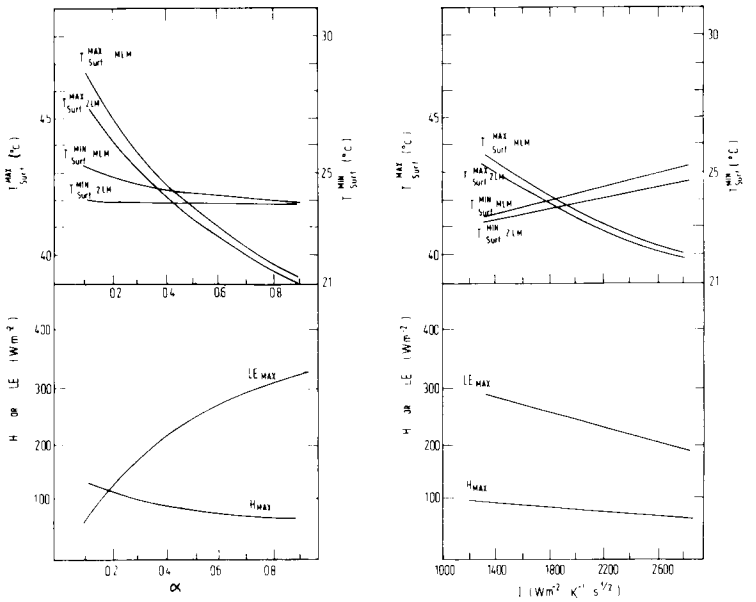

Fig. 2. Sensitivity of: surface temperature (extreme values) estimated by the multi-layer model (symbol MLM) and by the two-layer model (symbol 2LM) and fluxes H, LE estimated by the multi-layer model (maximum values) to humidity parameter α and thermal inertia I (August 7, 1979).

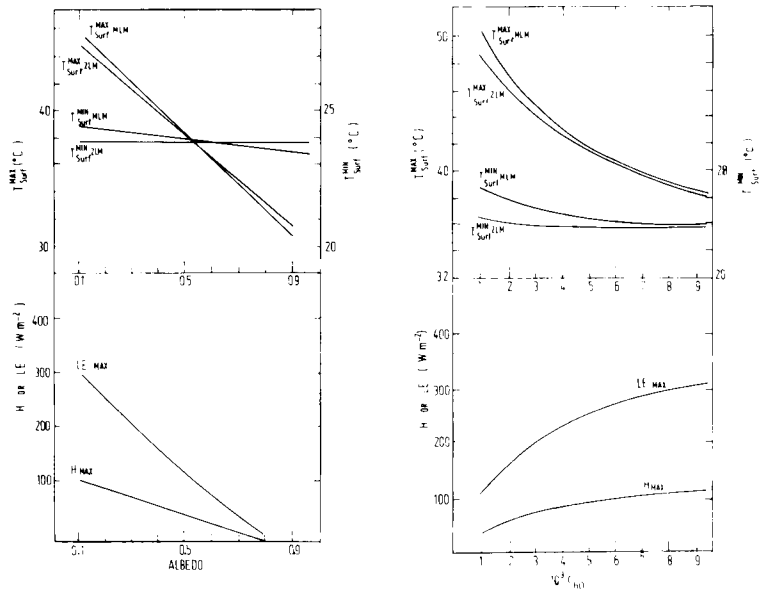

Fig. 3. Sensitivity of: surface temperature (extreme values) estimated by the multi-layer model (symbol MLM) and by the two-layer model (symbol 2LM) and fluxes H, LE estimated by the multi-layer model (maximum values) to albedo A and bulk coefficient C_{h0}.

corresponding minimum values are also represented. Moreover, we present the maximum values of fluxes H and LE issued from the multi-layer model. For a variation of the parameters around their initial values, an increase of 1 K in T_{surf}^{max} MLM is expected when:

A decreases by 0.1, or:

the thermal inertia I (equal to $\lambda\kappa^{1/2}$) is reduced by 400 W m^{-2} k^{-1} s$^{1/2}$, or:

α decreases by 0.1, or:

C_{h0} decreases by 10^{-3}.

As regards the surface emissivity ε_s (results not presented here), there was little sensitivity in the range of its possible values: the decrease is about 0.75 K when ε_s is increased from 0.80 to 1. The maximum T_{surf}^{max} 2LM varies approximately in the same way.

The latent heat flux seems more sensitive than the sensible heat flux. The responses of the maximum values of H and LE to changes in I, A and C_{h0} are similar: they decrease when I and A increase, or when C_{h0} decreases. On the other hand, when the parameter α increases, H decreases but LE increases, because the effect of a greater moisture at the surface overcomes the moderating effect of the decrease in the surface temperature.

The lowest soil layer temperature θ_∞ was also investigated. It moderately influences T_{surf}^{max} 2LM: an increase of about 0.25 K is observed when θ_∞ is increased by 1 K. On the other hand, in the same conditions, the multi-layer model is almost insensitive to θ_∞ for a 24-h run. When this value is not experimentally available, Blackadar (1976) stated that it could be estimated from the mean air temperature of the previous day. The last test concerned the effect of changes in κ and λ with constant I: only the inner layer temperatures are changed, but not the surface temperature, which is governed by thermal inertia. This is in agreement with the results of Carlson et al. (1981).

4. Verification of the models

4.1. Initialization of the models

Integration begins at 0 h (local time). For the empirical models, the initial surface temperature was chosen as the air temperature at the same hour. Great accuracy in this initial value is not required: after 2 h of simulated time, the calculated surface temperatures are not affected by the initial conditions, even for departures of several degrees in the initial temperature. After interpolation, the measured temperature profile at 0 h (local time) is used to initialize the multi-layer model. As there is experimental evidence that at 80 cm depth the temperature gradient is weak and the temperature itself varies very slowly, θ_∞ is assigned this experimental value of 0 h. Moreover, θ_∞ is not allowed to vary for a given day. (Experimentally, the changes did not exceed 0.1 K per day.) The same value of θ_∞ is used in the multi-layer model and in model 5. The multi-layer is not sensitive to variations of initial temperature in the upper soil layer (0–20 cm).

4.2. Adjustment of the basic parameters

This adjustment was performed using the multi-layer model. The parameters, one at a time, were modified so as to get a good fitting of the experimental values of the soil temperatures and of the fluxes by the multi-layer model. The modification of the basic parameters was performed with the help of the results of sensitivity runs. This adjustment may be described briefly as follows: for every day, the thermal inertia I was slightly modified and the model was run in order to get the theoretical curve θ_0 close to the experimental one. The C_{h0} was adjusted so as to get a good agreement for H. Finally, the wetness α was modified so as to get an acceptable curve for LE. At every step, if necessary, all the parameters already estimated in the previous steps could be slightly modified in order to preserve the fitting already fulfilled. If one of those steps could not be achieved, another value of albedo A was chosen and the complete cycle was re-run so as to get a good general agreement. The last step consisted in the choice of the best value of κ (or λ): for the value of I found in the first step, κ was modified (and λ) in order to get good agreement in the ground temperatures at the 10 cm and 20 cm levels. Due to the lack of sensitivity to this parameter, the emissivity ε_s was chosen equal to 0.9. All the test runs showed that the best value for C_{h0} was $5 \cdot 10^{-3}$. The hypothesis of constant C_{h0} is questionable, because this bulk coefficient is likely to be an increasing function of the instability in the atmospheric surface layer (Greenhut, 1982). Nevertheless, the behaviour of C_{h0} associated with weak wind speeds is not yet completely known, and for the purpose of the present study, a constant

value was selected (moreover, it is not easy to take the surface layer stability into account with the routine parameters we used here).

The goodness-of-fitting of calculations with experimental data was evaluated partly by eye, and partly by use of the following statistical parameters: let X represent the chronological set of any experimental variable (surface temperature or fluxes) for a given day, and Y the corresponding theoretical values. We have calculated:

the linear correlation coefficient r between X and Y;

the linear regression coefficients a and b for the relation $Y = aX + b$;

the mean square distance between X and Y:

$$d_{XY} = \left[\frac{\sum_i (X_i - Y_i)^2}{N} \right]^{1/2}, \tag{18}$$

where N is the length of the series X (or Y), i.e., the number of experimental (or theoretical) points of the function X (or Y); for a time step of 5 min, this number is 288. The parameter d_{XY} represents the error of the model estimations;

the normalized distance (or relative error):

$$\delta_{XY} = d_{XY}/A_X, \tag{19}$$

where A_X is the experimental range of X.

The values of the basic parameters we found by

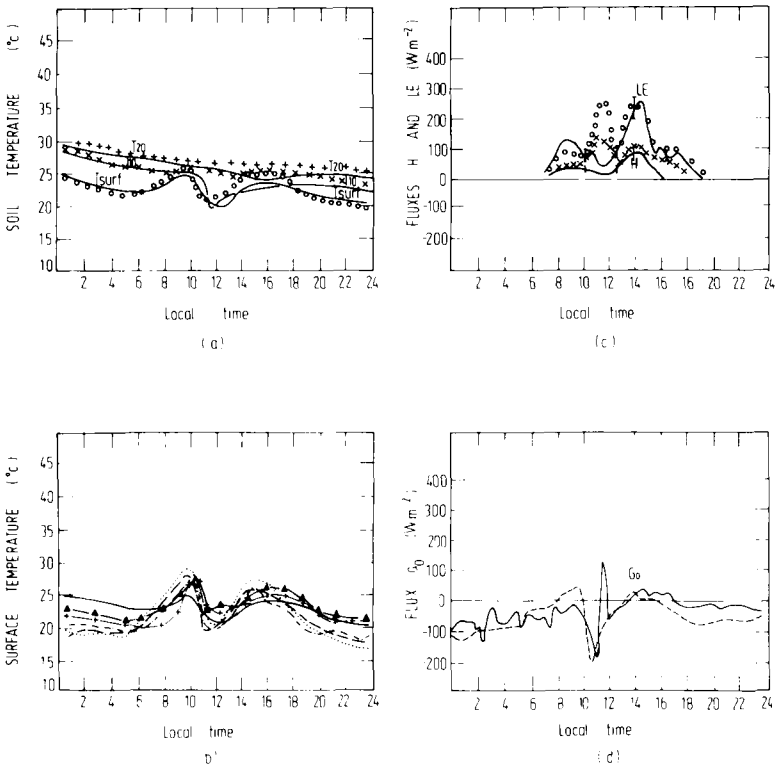

Fig. 4. Comparison of model results with experimental data (July 31, 1979). Curves a: surface temperature T_{surf} (experimental value: ——; calculated by the multi-layer model: o o o); T_{10}, temperature at 10 cm depth (experimental value: ——; calculated by the multi-layer model: × × ×); T_{20}, temperature at 20 cm depth (experimental value: ——; calculated by the multi-layer model: +++++). The experimental error in temperature is 0.1 K. Curves b: surface temperature T_{surf} (experimental value: ——; calculated by model 1: ....; model 2: – – – –; model 3: –·–·–·–; model 4: -+-+-+-+-; model 5: ▲–▲–▲–▲). Curves c: fluxes H and LE (H: experimental values: ——, calculated by the multi-layer model: × × ×; LE: experimental value: ——; calculated by the multi-layer model; OOO). Vertical dashes symbolize the experimental errors. Curves d: flux G_0 (experimental values: ——; calculated by the multi-layer model: – – – –).

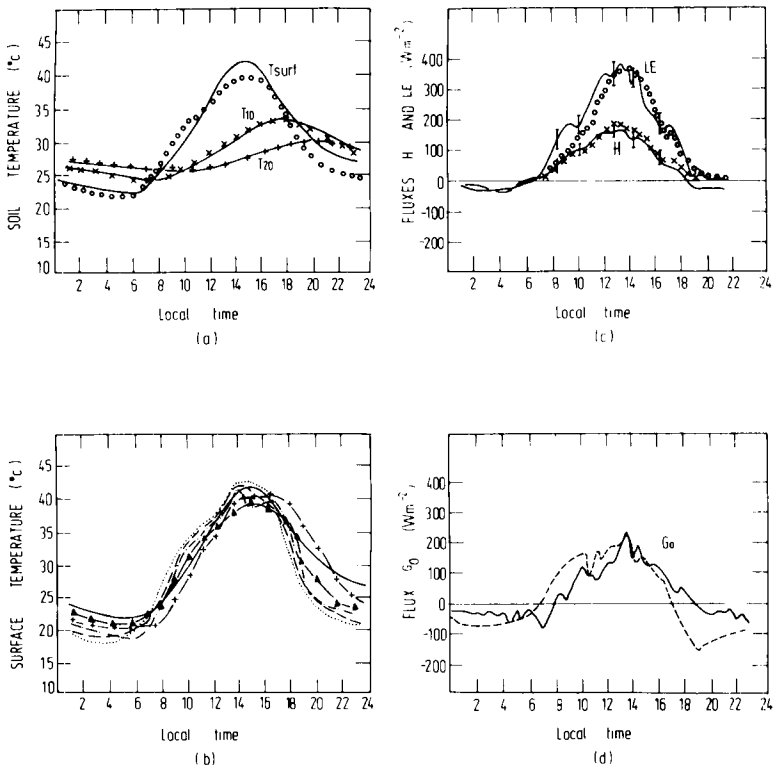

Fig. 5. Same as Fig. 4, but August 2, 1979.

these runs range between the following limits:

$1.50 < \lambda < 1.60$ (W m^{-1} K^{-1});

$0.65 \cdot 10^{-6} < \kappa < 0.80\ 10^{-6}$ (m^2 s^{-1});

$0.15 < A < 0.30$;

$0.40 < \alpha < 0.70$.

It may be noted that the range of the possible values for κ and λ is not very large.

4.3. Presentation of the result set

Figs. 4–6 present examples of calculations compared with experimental data for some typical days. On July 31, a squall line occurred in the morning (Fig. 4); August 2 and 10 were sunny (Figs. 5 and 6). Table 2 summarizes the statistical parameters for the multi-layer model: correlation and regression coefficients and distances between experimental and calculated values (i.e. the model errors) for the surface temperature, H and LE.

4.4. Temperatures from the multi-layer model

The surface temperatures issued from the multi-layer model are in rather good agreement with the experimental data (Figs. 4a, 5a and 6a). It may be noticed, however, that the nocturnal values are less satisfactory, probably because the bulk coefficient is overestimated by night: a lower value of C_{h0} would lead to lower absolute values of fluxes H and LE, which are negative by night. As the surface temperature governs sensible and latent heat exchanges, and these fluxes are very weak by night, accuracy in determining the surface temperature is much more necessary by day, when H and LE are high, than by night. The errors d_{XY} range between 1.05 and 2.5 K, with an average value of about 2 K. The correlation coefficients are satisfactory, except for July 31. On this day there was rainfall (24 mm) in the morning at 10 h (local time), but the model as presented here does not take rainfall into account. In Fig. 4a, the experimental curves, but not the theoretical curves, reveal an obvious cooling (particularly at 10 cm).

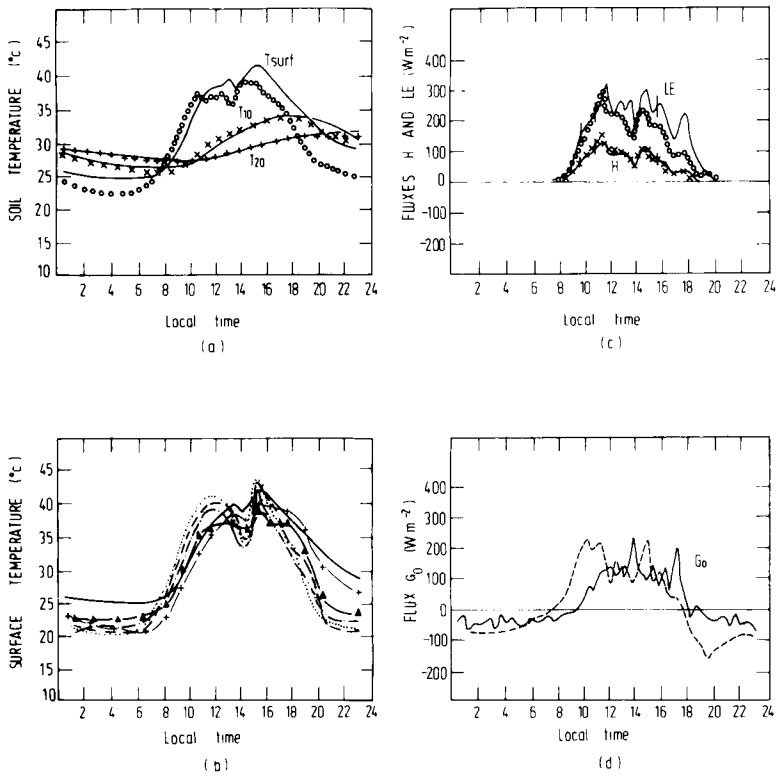

Fig. 6. Same as Fig. 5, but August 10, 1979.

Table 2. *Statistical results from comparison of multi-layer model with experimental data (soil parameters adjusted every day)*

		31-07	01-08	02-08	03-08	04-08	05-08	06-08	07-08	08-08	09-08	10-08
surface temperature	a	1.12	1.19	0.94	1.03	0.90	1.29	1.13	1.01	1.06	1.00	0.97
	b	−2.94	−5.02	0.98	−2.65	1.50	−8.27	−4.05	−1.34	−3.26	−1.68	−0.59
	r	0.83	0.98	0.96	0.91	0.97	0.94	0.97	0.95	0.94	0.97	0.95
	d_{XY}	1.05	1.45	2.11	2.80	2.40	1.56	1.65	1.99	2.10	2.14	2.48
	δ_{XY}	0.19	0.11	0.10	0.18	0.11	0.18	0.09	0.12	0.15	0.13	0.15
H	a	1.26	1.13	0.89	0.98	0.88	1.11	lack of experimental data	0.80	0.85	0.61	0.86
	b	14.1	20.3	16.9	14.4	17.4	18.4		12.6	7.80	15.1	13.3
	r	0.84	0.85	0.98	0.93	0.95	0.89		0.95	0.98	0.93	0.96
	d_{XY}	19.0	28.4	18.5	22.6	18.9	21.3		14.5	11.4	24.3	16.2
	δ_{XY}	0.28	0.24	0.09	0.16	0.17	0.26		0.12	0.07	0.12	0.10
LE	a	0.86	0.99	0.88	0.78	1.03	0.98		0.90	0.85	0.81	0.75
	b	15.81	−1.57	6.52	8.67	2.29	19.9		8.05	−0.25	5.87	4.92
	r	0.83	0.97	0.98	0.98	0.93	0.94		0.94	0.99	0.97	0.97
	d_{XY}	23.9	22.1	29.8	31.9	25.5	27.2		26.6	27.5	27.5	37.5
	δ_{XY}	0.17	0.08	0.09	0.08	0.14	0.11		0.11	0.07	0.07	0.11

As regards the surface temperature, it is important to keep in mind that the experimental parameter considered to represent it, is merely the output of the thermal gauge at depth zero, i.e. lying straight on the ground and covered with a fraction of millimeter of earth. Direct measurement of the exact boundary temperature—the so-called "skin temperature"—is not possible. This parameter results from various processes (conductive, convective and radiative), unlike the temperature in any inner layer of the soil, which proceeds, neglecting water transfer in the ground, from conductive processes only. Radiometric measurements of surface temperature (from aircraft or satellite) would be more relevant on theoretical grounds, but during this phase of the experiment, no accurate available data exist. As a matter of fact, surface temperature calculations by models take the aforementioned processes into account. Thus, they are somewhat connected with radiometric temperatures. The calculations, however, agree with the experimental data. Temperatures at 10 cm and at 20 cm also closely agree. Theoretical and experimental curves appear much smoother than surface curves. This fact may be easily explained: the surface temperature may be represented, as it is a quasi-periodic function of time, by a sum of pure harmonic waves of increasing frequencies. The higher frequencies' contributions (originating, say, from rapid changes in cloudiness, see e.g. Fig. 6a) may be important. Now, the damping of a thermal wave of frequency f with the vertical coordinate z is proportional to $\exp(-Kf^{1/2}z)$, where K is a constant depending only on the type of soil (Carslaw and Jaeger, 1978). Thus, the high-order harmonics are quickly attenuated with increasing z: the soil acts as a low-pass filter. This softening of the shape of curves is confirmed by experiment, and the model accounts for it too.

4.5. Fluxes H and LE from the multi-layer model

On the curves of Figs. 4c to 6c, the nocturnal values are generally omitted because they are weak (about some W m^{-2}) and highly fluctuating, with theoretical as well as experimental values (the nocturnal values of wind velocities do not allow a high accuracy in flux determination by the aerodynamic method). Table 2 shows that the mean values of the square distances (errors) for H and LE are 20 W m^{-2} and 28 W m^{-2}, respectively, i.e. 16% and 10% in relative values. The latent heat flux seems more accurately calculated than the sensible heat flux. High-frequency fluctuations of measured fluxes may be noticed in model issues also. The correlation coefficients are high, with lower values on the days with squall lines, i.e. July 31 and August 5.

4.6. Surface soil heat flux G_0

It is obvious from Figs. 4d to 6d that the agreement between theoretical and experimental G_0 values is less satisfactory than for H and LE. Particularly, a phase lag of the experimental curve with respect to the theoretical one may often be observed. This lag is about 1–2 h. Depending on the day, the correlation coefficient may vary between the limits 0.65 and 0.83. We did not present here the experimental errors on G_0, because, in the determination of this flux, the specific heat C was not measured directly (see Section 3): thus, the errors on the vertical profile of C are not available. It is realistic, however, to state that these experimental errors could not account thoroughly for the departures between experimental and theoretical values: their somewhat systematic character as well as the shape of theoretical curves suggests that they originate more from the model itself.

4.7. Surface temperatures from the empirical models

These models use the same values of the basic physical parameters as the multi-layer model. Figs. 4b to 6b show the surface temperature from the empirical models. Since it governs the fluxes H and LE, the accuracy of these models may be evaluated by examination of this parameter. For this reason, the fluxes H and LE calculated by the empirical models are not presented here. All of these models provide results markedly different from the experimental data, except model 5. This two-layer model provides issues surprisingly comparable with those of the more complex multi-layer model.

5. Two supplementary tests

5.1. A run with constant basic parameters

Table 3 refers to a run for which the basic parameters κ, λ, A and α (and, of course, ε_s and C_{h0}) were kept constant over the whole period of 11

Table 3. *Statistical results from comparison of multi-layer model with experimental data (soil parameters hold constant over the whole period)*

		31-07	01-08	02-08	03-08	04-08	05-08	06-08	07-08	08-08	09-08	10-08
surface temperature	a	0.92	1.21	0.85	0.96	0.96	1.42	1.19	1.06	1.06	1.02	0.95
	b	0.15	−5.42	2.68	−1.72	−0.25	−12.8	−5.61	−3.44	−3.93	−2.72	−0.81
	r	0.64	0.97	0.96	0.91	0.96	0.88	0.97	0.95	0.95	0.97	0.96
	d_{XY}	2.28	1.71	2.65	3.44	2.55	2.82	1.89	2.42	2.57	2.54	3.04
	δ_{XY}	0.42	0.13	0.13	0.22	0.11	0.32	0.11	0.14	0.18	0.15	0.18
H	a	1.34	1.23	0.74	0.79	1.00	1.39	lack of experimental data	0.88	0.78	0.60	0.76
	b	1.07	22.9	11.7	4.87	16.1	6.23		6.14	1.61	10.2	7.85
	r	0.87	0.86	0.98	0.91	0.95	0.91		0.95	0.97	0.91	0.96
	d_{XY}	11.9	31.7	19.7	19.0	19.9	15.6		11.0	13.0	24.4	15.1
	δ_{XY}	0.17	0.27	0.10	0.13	0.18	0.19		0.09	0.08	0.12	0.10
LE	a	0.82	0.90	0.88	0.78	1.45	1.00		0.95	0.76	0.80	0.81
	b	−10.7	−0.55	4.35	−2.77	−2.91	14.6		−3.04	−9.40	−2.77	0.14
	r	0.81	0.97	0.98	0.97	0.93	0.94		0.94	0.99	0.96	0.97
	d_{XY}	25.3	24.6	30.2	39.2	50.4	23.3		28.5	42.1	32.5	33.9
	δ_{XY}	0.18	0.09	0.09	0.09	0.28	0.10		0.11	0.11	0.09	0.10

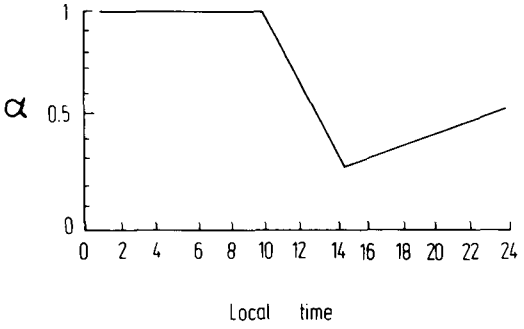

Fig. 7. Variation of α during daytime for the simulation of drying of the upper soil layers.

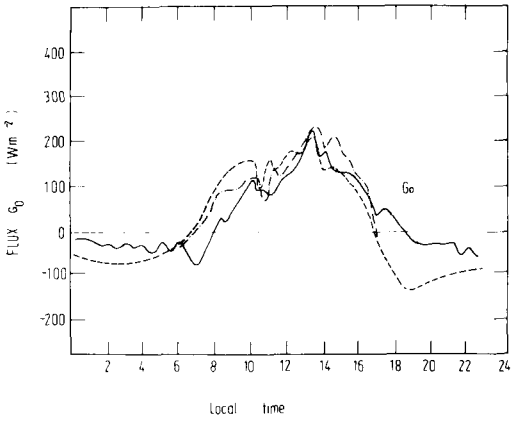

Fig. 8. A simulation of soil surface drying during daytime. Effect on G_0 (experimental G_0: ——; calculated with constant α: – – – –; with variable α –·–·–·–) (August, 2).

days. The values chosen are $\lambda = 1.55$ W m^{-1} K^{-1}; $\kappa = 0.7\ 10^{-6}$ m^2 s^{-1}; $A = 0.20$; $\alpha = 0.40$, which are crudely the mean values of those relative to the previous case. This run shows slightly more important deviations, but the correlation coefficients remain the same. This trial simulates the use of surface models with seasonal values of the physical parameters.

5.2. *Use of a variable wetness parameter*

In Subsection 4.6 are pointed out some discrepancies between theoretical and experimental values of G_0. These may result from the assumption that the soil properties are constant. A run with α taken as a function of time has been performed. Drying of the upper soil layers during the first part of the day is simulated by assigning to α a decreasing value from 10 a.m. to 2 p.m. (local time). Afterwards, α begins to grow slowly again (which accounts for wetness restoration in the upper layers by capillarity from the lower layers).

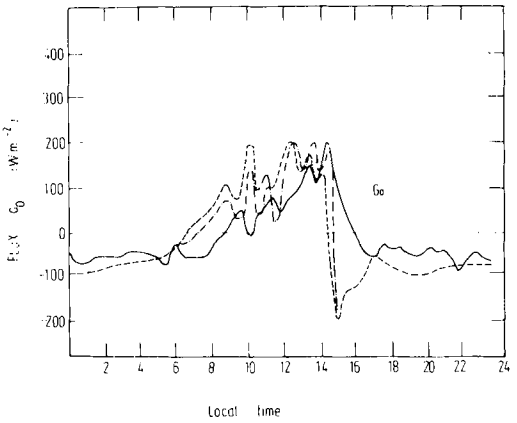

Fig. 9. A simulation of soil surface drying during daytime. Effect on G_0 (experimental G_0: ——; calculated with constant α: – – – –; with variable α: –·–·–·–) (August, 3).

Fig. 7 presents this variation. The lag seems somewhat less important (Figs. 8 and 9). For this trial, coupling between soil wetness and κ (or λ) has been neglected. The assumption that the soil parameters are uniform precludes such a simulation. Moreover, eq. (11) would no longer be satisfactory and would have to be replaced by the following:

$$C(z)\frac{\partial\theta}{\partial t} = \frac{\partial}{\partial z}\left[\lambda(z)\frac{\partial\theta}{\partial z}\right]. \qquad (20)$$

6. Conclusions

Various models estimating the energy fluxes at the soil-atmosphere interface have been tested against experimental data in the tropical zone during the rainy season. The purpose of this study was an evaluation of errors involved by current assumptions generally emphasized in large-scale models for soil surface properties: bare surface and constant and uniform physical properties of the ground. The surface parameters have not been measured on the experiment site, but adjusted for every day by test runs. Some of them, such as thermal conductivity or diffusivity, did not have great variability from one day to the next. The tests showed that it was possible to use surface models with a set of surface properties kept constant over a period of several days, with different meteorological conditions, without involving any marked increase in errors. Relative errors in the evaluation of H and LE by the multi-layer model are only a small % greater than in the case of the daily adjustment of the parameters. Bulk evaluation of the energy fluxes is therefore fairly realistic, at least the diurnal period, and whatever the meteorological conditions (sunny or disturbed) may be.

Estimates of surface soil heat flux G_0 are not as accurate as for H and LE. The correlation coefficients are about 20% lower, and the relative errors about twice as important as in the case of LE. Except for the two-layer model, empirical models lead to rather irrelevant results.

Such a direct attempt at qualifying surface models is a contribution to the study of the sensitivity of large-scale models to surface conditions. Further numerical tests are necessary for investigating the conditions of accuracy in surface data (temperature and energy fluxes) for which the feedback between larger scale and ground surface models can lead to non-divergent running. More precisely, it is necessary to investigate how errors in fluxes at the soil-atmosphere interface influence the quality of the predictions by the large-scale models. If one can tolerate errors of about 10% of 20%, it is possible to use with constant ground properties a simple model such as the multi-layer or even the two-layer model. This two-layer model is of large use and models such as the NCAR GCM or the "Modèle Améthyste Tropical" of the Météorologie Nationale Française (Assamoi, 1984a; Assamoi, 1984b) include it. Otherwise, assumptions about soil properties should be improved.

7. Acknowledgements

The authors wish to thank Professor Soulage and Doctor Isaka (Laboratoire Associé de Météorologie Physique, Université de Clermont-Ferrand) and also Professor Baudet and Professor Achy (Laboratoire de Physique de l'Atmosphère, Université d'Abidjan) for helpful discussions as well as material assistance for this study.

8. List of symbols

A ground surface albedo.
C specific heat of soil.
C_1 a constant used in cloudiness formulation ($C_1 = 0.8$).
C_{h0} bulk aerodynamic coefficient for heat and water vapour transfer.

C_p specific heat of air at constant pressure.
d_1 parameter representing an order of magnitude of soil thickness under influence of the diurnal temperature variation, $d_1 = (\kappa\tau)^{1/2}$.
$\bar{e}_a$ mean value (at daytime scale) of e_a (air vapour pressure).
$e_{sat}(T)$ saturation vapour pressure at temperature T.
G_0 surface soil heat flux.
H sensible heat flux (surface value).
I soil thermal inertia ($I = \lambda\kappa^{-1/2}$).
L latent heat of evaporation for water.
LE latent heat flux (surface value).
q_a specific humidity at level 2 m.
q_0 specific humidity for air at ground surface.
$q_{sat}(T)$ saturation specific humidity at temperature T.
R_{IR} net IR budget at ground surface.
R_G global radiation at surface level.
R_{G0} global radiation at surface level with clear sky.
R_L atmospheric downward IR radiation.
R_N net radiation at ground surface level.
R_T IR radiation emitted by soil surface.
T_a dry bulb thermometer temperature at level 2 m.
$\bar{T}_a$ mean value (at daytime scale) of T_a.
T_h wet bulb thermometer temperature at level 2 m.
T_{surf}, T_{10} and T_{20} temperatures at depths 0, 10 and 20 cm (symbols used in Figs. 4 to 6).
T_{surf}^{max} MLM maximum value of the surface temperature (evaluated with the multi-layer model).
T_{surf}^{max} 2LM maximum value of the surface temperature (evaluated with the two-layer model).
t time.
Δt time step in discretized equations.
u_a wind speed at level 2 m.
z vertical coordinate (positive upwards; origin 1 m depth).
α adimensional humidity parameter for soil surface (lying between 0 and 1).
ε_s surface emissivity.
$\theta(z, t)$ thermal profile in the soil (theoretical values).
$\theta_e(z, t)$ thermal profile in the soil (experimental values).
θ_0 soil surface temperature.
θ_∞ soil temperature at the lower limit of the integration grid.
κ thermal diffusivity for soil $= \lambda/C$.
λ thermal conductivity of soil.
ν cloudiness.
ρ_a air density at level 2 m.
σ the Stefan constant
τ diurnal period.

REFERENCES

Assamoi, P. 1984a. Numerical weather forecasting in western Africa: influence of sub-grid scale parametrization on forecasting efficiency. (In French: "Prévision numérique du temps en Afrique de l'Ouest: influence de la paramétrisation de processus "sous-maille" sur la performance des modèles de prévision".) Thèse de Doctorat ès-Sciences Physiques n°. 78, Université d'Abidjan, Ivory Coast.

Assamoi, P. 1984b. Numerical investigation of west African disturbances during monsoon. (In French: "Etude numérique des perturbations sur la région Ouest-Africaine en période de mousson".) *Journal de Recherches Atmosphériques 2*, 81–94.

Blackadar, A. K. 1976. Modeling the nocturnal boundary layer. *Proc. of the Third Symposium of Atmospheric Turbulence, Diffusion and Air Quality*, Amer. Meteorol. Soc., Boston, 46–49.

Budyko, M. I. 1974. *Climate and life*. Academic Press, New York.

Carlson, T. N., Dodd, J. K., Benjamin, S. G. and Cooper, J. N. 1981. Satellite estimation of the surface energy balance, moisture availability and thermal inertia. *J. Appl. Meteorol. 20*, 67–87.

Carslaw, H. S. and Jaeger, J. C. 1978. *Conduction of heat in solids*. Oxford University Press (2nd edition).

Coulibaly, Y. 1981. Local behaviour of heat and mass surface fluxes at several time scales in the tropical region (during WAMEX 1979). (In French: "Evolution locale à différentes échelles de temps des flux de chaleur et de masse en zone tropicale (période WAMEX 1979)".) Thèse de Troisième Cycle n°. 663. L.A.M.P., Université de Clermont-Ferrand, France.

Deardorff, J. W. 1978. Efficient prediction of ground surface temperature and moisture with inclusion of a layer of vegetation. *J. Geophys. Res. 83*, 1889–1903.

De Vries, D. A. 1966. Thermal properties of soils. In: *Physics of plant environment* (ed. W. R. Van Wijk). North Holland, Amsterdam, 210–235.

Greenhut, G. K. 1982. Stability dependance of fluxes and bulk transfer coefficients in a tropical boundary layer. *Boundary Layer Meteorol. 24*, 253–264.

Hervier, R., Soulage, M. and Barthout, J. L. 1979. The

L.A.M.P. automatic micrometeorological station for surface energy budget measurements. (In French: "Station micrométéorologique automatique du L.A.M.P. pour la mesure du bilan énergétique du sol".) Technical report n°. 24. L.A.M.P., Université de Clermont-Ferrand, France.

Laval, K., Sadourny, R. and Serafini, Y. 1978. Soil surface energy and water budgets formulation in a general circulation model. (In French: "Formulation des bilans énergétique et hydrologique à la surface du sol, dans un modèle de circulation générale".) Reprint of the National Colloquium on "Mécanismes de Transfert d'énergie et de masse entre Sol et Atmosphère" (A.S.P. Evolution des climats CNRS-DGRST) (ed. F. Becker and C. Pastre), 1–40.

Paltridge, G. W. and Platt, L. M. R. 1978. Radiative processes in meteorology and climatology. *Developments in atmospheric sciences*, 5. Elsevier Scientific Publishing Company, Amsterdam, The Netherlands.

Reed, R. K. and Halpern, D. 1975. Insolation and net long-wave radiation of the Oregon coast. *J. Geophys. Res. 80*, 839–844.

Rockwood, A. A. and Cox, S. K. 1978. Satellite-inferred surface albedo over northwestern Africa. *J. Atmos. Sci. 35*, 513–522.

Saugier, B. and Ripley, E. A. 1978. Evaluation of the aerodynamic method of determining fluxes over natural grassland. *Q. J. R. Meteorol. Soc. 104*, 257–270.

Washington, W. M. and Williamson, D. L. 1977. A description of the NCAR global circulation models. *Methods Comput. 17*, 111–172.

Zhang, D. and Anthes, R. A. 1982. A high-resolution model of the planetary boundary layer—sensitivity tests and comparisons with the SESAME-79 data. *J. Appl. Meteorol. 21*, 1594–1609.